THE STRUCTURAL DESIGN OF TALL AND SPECIAL BUILDINGS
Struct. Design Tall Spec. Build. **16**, 615–632 (2007)
Published online in Wiley Interscience (www.interscience.wiley.com). **DOI**: 10.1002/tal.440

MODELLING ISSUES FOR TALL REINFORCED CONCRETE CORE WALL BUILDINGS

JOHN W. WALLACE*
Department of Civil & Environmental Engineering, University of California, Los Angeles, California, USA

SUMMARY

Reinforced concrete walls are commonly used as the primary lateral force-resisting system for tall buildings. As the tools for conducting nonlinear response history analysis have improved and with the advent of performance-based seismic design, reinforced concrete walls and core walls are often employed as the only lateral force-resisting system. Proper modelling of the load versus deformation behaviour of reinforced concrete walls and link beams is essential to accurately predict important response quantities. Given this critical need, an overview of modelling approaches appropriate to capture the lateral load responses of both slender and stout reinforced concrete walls, as well as link beams, is presented. Modelling of both flexural and shear responses is addressed, as well as the potential impact of coupled flexure–shear behaviour. Model results are compared with experimental results to assess the ability of common modelling approaches to accurately predict both global and local experimental responses. Based on the findings, specific recommendations are made for general modelling issues, limiting material strains for combined bending and axial load, and shear backbone relations. Copyright © 2007 John Wiley & Sons, Ltd.

1. INTRODUCTION

Reinforced concrete (RC) structural walls are effective for resisting lateral loads imposed by wind or earthquakes. They provide substantial strength and stiffness as well as the deformation capacity needed to meet the demands of strong earthquake ground motions. As the tools for conducting nonlinear response history analysis have improved and the application of performance-based seismic design approaches have become common, use of reinforced concrete walls and core walls for lateral force resistance along with a slab-column gravity frame have emerged as one of the preferred systems for tall buildings.

The lateral force-resisting system for a building is sometimes concentrated in relatively few walls distributed around the floor plate or within a central core wall to provide the lateral strength and stiffness needed to limit the lateral deformations to acceptable levels. Although extensive research has been carried out to study the behaviour of reinforced concrete walls and frame wall systems, including development of very refined modelling approaches, use of relatively simple or coarse models is required for very tall buildings to reduce computer run times associated with nonlinear response history analyses. Therefore, it is important to balance model simplicity with the ability to reliably predict inelastic responses both at the global and local levels under seismic loads to ensure that the analytical model reasonably represents the hysteretic response of the primary lateral force-resisting elements (including the foundation), as well as the interaction between the wall and other structural (gravity) members.

*Correspondence to: John W. Wallace, Department of Civil & Environmental Engineering University of California, Los Angeles, CA, USA. E-mail: wallacej@ucla.edu

The most common modelling approach used for RC walls involves using a fibre beam-column element (e.g, PERFORM 3D, 2006) or the Multiple-Vertical-Line-Element (MVLE) model, which is similar to a fibre model (Orakcal and Wallace, 2006). Use of either of these models allows for a fairly detailed description wall geometry, reinforcement and material behaviour, and accounts for important response features such as migration of the neutral axis along the wall cross-section during loading and unloading, interaction with the connecting components such as slab-column frames and coupling/outrigger beams, both in the plane of the wall and perpendicular to the wall, as well as the influence of variation of axial load on wall flexural stiffness and strength. Important modelling parameters include the definition of the material properties for the longitudinal reinforcement, the core concrete enclosed by transverse reinforcement (i.e., confined concrete), and cover and web concrete (i.e., unconfined concrete). A more complex model and material behaviour can also be described that incorporates observed interaction between flexural/axial behaviour and shear behaviour (Massone *et al.*, 2006; Orakcal *et al.*, 2006); however, an uncoupled model, where flexure/axial behaviour is independent of shear behaviour, is commonly used for design.

Coupling or link beams commonly exist due to the core wall configuration, or they are needed to enhance the lateral stiffness of the building, and proper modelling of the load versus deformation behaviour of coupling beams is essential to accurately predict important response quantities. Selection of appropriate flexural stiffness values for the coupling beams is particularly important as it impacts the degree of coupling between walls as well as the coupling beam shear stress. Use of a value equal to one-half of the gross concrete section inertia is commonly recommended (e.g., FEMA 356, 2000); however, use of this value generally produces higher shear stresses than are acceptable for design. Given this problem, it is common practice to reduce coupling beam stiffness to significantly lower values, on the order of $0{\cdot}25I_g$ to $0{\cdot}15I_g$, or less, to achieve an acceptable level of shear stress for the design forces. At issue is whether this level of stiffness reduction for the design basis earthquake produces excessive concrete spalling that could be dangerous, and what level of stiffness reduction is appropriate for a service level check (e.g., 50% in a 30-year event).

It is common for the footprint of the building at the lower levels to be larger than the tower footprint to accommodate parking and retail needs. This abrupt change in geometry can have a significant impact on the distribution of lateral forces in the region of the discontinuity, where loads are shared between the core wall and the perimeter retail and basement level walls. Parking level walls are typically stout, i.e. the wall height-to-length or aspect ratio is low; therefore, selection of the stiffness values for flexure and shear is important and can substantially impact the distribution of lateral forces between the core wall and perimeter basement level walls. Since the floor slabs in the region of the discontinuity are required to transfer forces from the core wall to the perimeter walls, selection of appropriate slab stiffness values and design of slab reinforcement are important issues. Variation of slab and wall stiffness values is typically required to determine the potential range of design values to ensure proper design. For embedded basement levels, response history analysis is further complicated by the need to define the level at which the ground acceleration records are applied.

Slab-column frames, with its limited forming, low-story heights and open floor plan are an efficient system to resist gravity loads. The slab-column frame is typically designed to resist only gravity loads; however, the ability of the slab-column gravity frame to maintain support for gravity loads under the lateral deformations imposed on it by the lateral force-resisting system must be checked. The primary objectives of this 'deformation compatibility' check are to verify that slab-column punching failures will not occur for service-level and design-level earthquakes, as well as to assess the need to place slab shear reinforcement adjacent to the column to enhance slab shear strength. New design requirements for these checks are included in ACI 318-05 §21.11.5 (ACI, 2005). Detailing of the slab-wall connection is also an important design consideration, as the rotation of the core wall can impose relatively large rotation demands on the slab at the slab-wall interface (Klemencic *et al.*, 2006). Slip

DOI: 10.1002/tal

forming of the core wall is common to reduce construction time, requiring special attention to slab shear and moment transfer at the slab-wall interface.

As noted in the preceding paragraphs, design of tall buildings utilizing reinforced concrete walls is complicated by the uncertainty associated with a variety of issues. Although analytical modelling studies and experimental studies are appropriate for improving our understanding of some issues (e.g., coupling beams), it is clear that other issues can only be answered by installation of sensors in actual buildings. Ideally, the sensors could be installed both during and after building construction to enable the broadest spectrum of data collection and follow-up analytical studies. Sensors to measure a wide variety of response quantities (acceleration, force/pressure, velocity, displacement, rotation and strain) could be installed to collect critical data to improve our ability to model the dynamic responses of tall buildings. Data collection in ambient, wind, low-level earthquakes, as well as the significant earthquakes would help improve our modelling capabilities, and ultimately the economy and safety of tall buildings.

The preceding paragraphs provide an overview of several important issues associated with analysis and design of tall reinforced concrete buildings. A more detailed discussion, including a review of relevant recent research and specific recommendations, are presented in the following sections.

2. WALL MODELLING

Orakcal and Wallace (2006) present the most comprehensive study available on the ability of current modelling approaches to capture the cyclic response of relatively slender reinforced concrete walls for combined bending and axial load. An MVLE model, which is conceptually the same as the fibre model approaches that are embedded in some commercially available computer programs (e.g., PERFORM 3D), is employed in their study for walls subjected to reversed, cyclic, uni-axial loading. Given the wall cross-section and the quantity of longitudinal and transverse reinforcement, the overall process presented by Orakcal and Wallace (2006) involves: (a) subdividing the wall cross-section into unconfined concrete fibres, confined concrete fibres and reinforcement fibres; (b) selecting appropriate material relations; (c) subdividing the wall into a specified number of elements (components) over the wall height; (d) defining appropriate boundary conditions; and (e) imposing a prescribed load/displacement history. Some of the results of their study are shown in Figure 1 for a test of a 12-foot tall wall with a 4-inch by 48-inch cross-section subjected to constant axial load and reversed cyclic lateral displacements at the top of the wall. The test walls were approximately one-fourth scale models of prototype walls proportioned using the 1991 Uniform Building Code (Thomsen and Wallace, 1995, 2004).

It is noted that Orakcal and Wallace (2006) reduced the test data into lateral force versus deformation relations for flexure and shear. As well, spurious contributions from foundation rotation or slip between the test wall foundation and the strong floor were removed. Several important observations can be gleaned from the results. The effective linear stiffness to the yield point is very close to the $0{\cdot}5EI_g$ value commonly used for design (Figure 1(b)) and that the wall lateral load capacity computed using the nominal moment capacity at the wall critical section located at the wall base for as-tested material properties is slightly less than the maximum lateral load achieved during the test (Figure 1(a); Thomsen and Wallace, 2004). Results from a recent shake table test of a full-scale rectangular wall (Panagiotou and Restrepo, 2007) suggests a lower effective stiffness, on the order of $0{\cdot}2EI_g$ (Maffei, 2007); however, it is important to note that this test was conducted for relatively low axial load ($>0{\cdot}05A_g f'_c$) and it is not apparent whether the test data were processed to separate responses into flexural and shear load versus deformation behaviour or to account for any deformation contributions due to foundation flexibility. More importantly, a primary objective of the shake table test was to demonstrate that satisfactory lateral load behaviour could be achieved using approximately one-half

DOI: 10.1002/tal

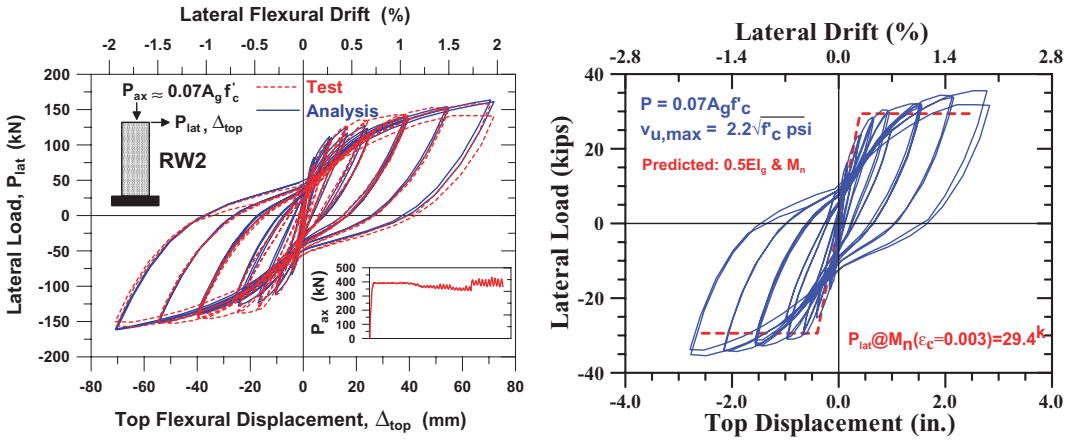

(a) Model results (Orakcal and Wallace, 2006) (b) Bilinear fit for $0.5EI_g$ and M_n

Figure 1. Test results for specimen RW2

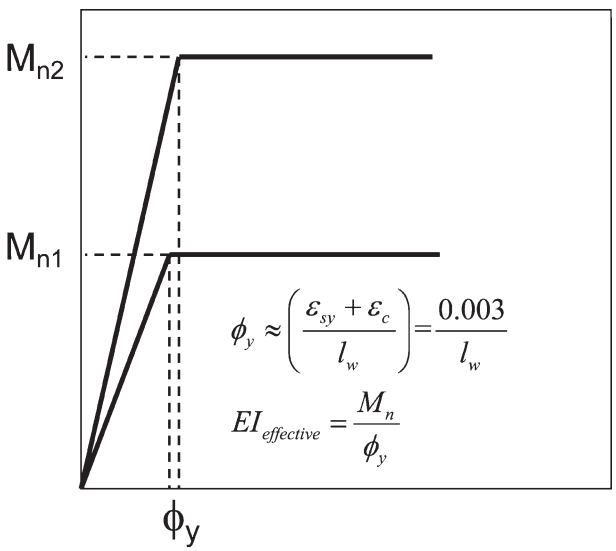

Figure 2. Wall effective stiffnes

the longitudinal reinforcement typically required by current codes in similar walls (e.g., UBC-97, 1997 or IBC-2003, 2003). Although a detailed assessment of the impact of the quantity of reinforcement used has not been conducted herein, it is noted that the tension reinforcement ratio for the shake table test $\rho_{bounday} = (8(0{\cdot}31\,\text{in}^2))/(8''(144'')) = 0{\cdot}0022$ is less than one-half of that used by Thomsen and Wallace (2004): $\rho_{bounday} = (8(0{\cdot}11\,\text{in}^2))/(4''(48'')) = 0{\cdot}0046$. Use of substantially lower longitudinal reinforcement would be expected to significantly impact the effective stiffness to yield because the yield curvature is primarily a function of the wall length, i.e. $\phi_y \approx (0{\cdot}0025 \text{ to } 0{\cdot}003)/l_w$ is commonly assumed (Wallace and Moehle, 1992). Therefore, for a given wall length, a reduction in the nominal (yield) moment strength by a factor of two will produce an approximately equal reduction in the effective stiffness (Figure 2). Given this result, the effective stiffness of $0{\cdot}2EI_g$ reported for the

DOI: 10.1002/tal

shake table test is not inconsistent with the results given in Figure 1. As more archived test results become available, a more detailed assessment of effective stiffness would be appropriate; however, until a more thorough assessment is conducted, continued use of an effective linear stiffness of $0{\cdot}5EI_g$ is appropriate for walls with code compliant strength and axial stress levels up to approximately $0{\cdot}15A_g f'_c$. For cases with substantially less boundary reinforcement (flexural strength) than required by current codes, use of a lower value might be appropriate. For higher levels of axial stress, use of a higher value may be justified; however, there are insufficient test data available to assess this case. It is noted that when a fibre element model is used, selection of effective flexural stiffness values is not possible, since the effective stiffness is 'automatically' determined based on the selected material relations, level of axial load and the current state (including history for nonlinear response history analysis).

The results presented also indicate that cyclic material relations for concrete and reinforcing steel can be selected to produce overall load versus deformation responses which are generally consistent with test results for a wide range of responses (i.e., overall load versus roof displacement, plastic hinge rotation and average strains). Orakcal and Wallace (2006) report that model and test results for first story displacements and rotations, where inelastic deformations dominate over elastic deformations, compare very favourably. Results for average wall strain over a nine-inch gauge length at the base of the wall (Figure 3) reveal that tensile strains are well represented with the model; however, model compressive strains substantially under estimate the peak compressive strains measured for several tests. In general, for the relatively slender wall tests ($h_w l_w = M_u/(V_u l_w) = 3$), peak measured compressive strains were about twice the model predicted strains. Therefore, until more information is available (test and model), limits placed on maximum compressive strains derived from model predictions should be doubled to compare with acceptance values for compressive strain (or the limit should be halved to compare with model strain values). Preliminary analytical studies have indicated that one reason for this discrepancy may be the interaction that occurs between flexural and shear behaviour, which is discussed in the following paragraph.

The results presented in Figures 1 and 3 represent nonlinear flexural behaviour. In cases where nonlinear flexural responses occur, linear shear behaviour is typically assumed, i.e. flexural behaviour and shear behaviour are uncoupled. It is apparent from the experimental results presented in Figure 4 for first story deformations that significant inelastic shear deformations initiate at the same applied lateral load as inelastic flexural deformations, i.e. the flexural and shear responses are coupled. The results presented in Figure 4 are for a wall with nominal shear capacity of approximately 300 kN; therefore,

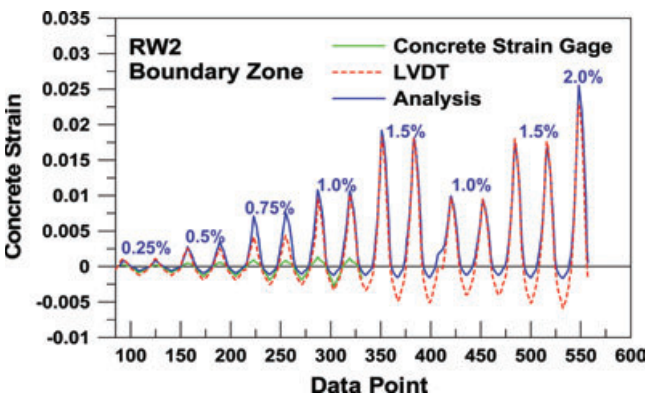

Figure 3. Wall average strain at critical section

DOI: 10.1002/tal

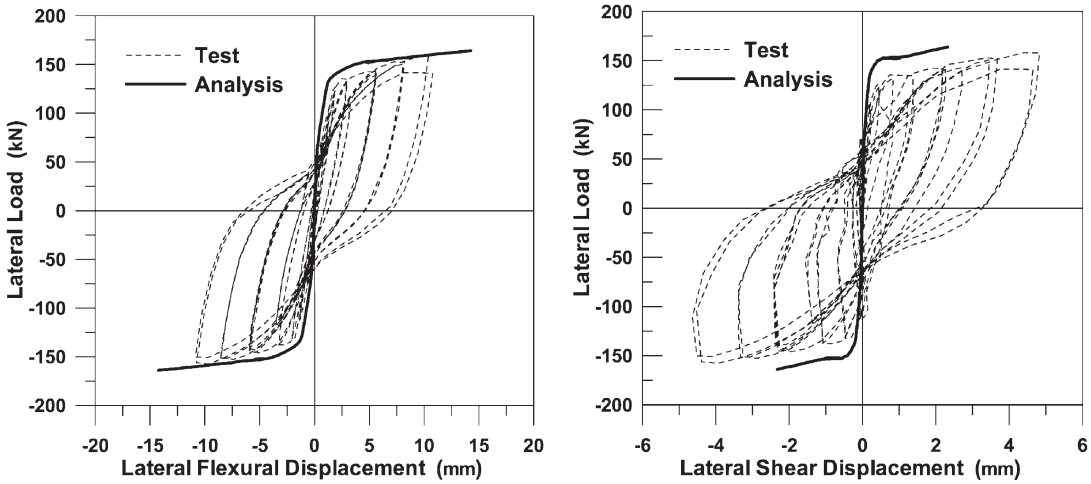

Figure 4. Load displacement relations: (a) flexure, (b) shear

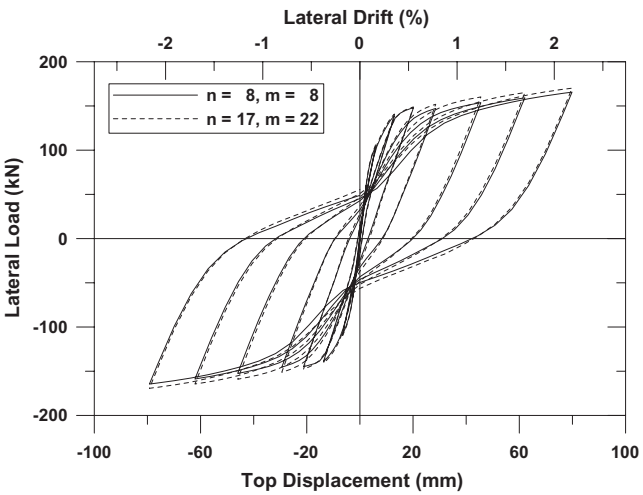

Figure 5. Load displacement model parameter sensitivity

for an uncoupled model, linear shear behaviour would be assumed. It is noted that currently available computer programs do not include models that account for the coupling of flexure and shear behaviour observed in Figure 4. The analysis results presented in Figure 4 are for a coupled model for monotonic material behaviour (Massone *et al.*, 2006a, 2006b), and they reveal that a coupled model can reproduce observed test results reasonably well. However, models that account for coupled flexure–shear behaviour for *cyclic* loading are not yet available in commercially available computer programs as development of coupled cyclic material models remains a significant research challenge.

Determination of an appropriate model for nonlinear response analysis requires subdividing both the cross-section into concrete and steel fibres, and subdividing the overall wall into elements of appropriate heights to capture salient responses. Results presented in Figure 5 reveal that a lateral load

DOI: 10.1002/tal

versus lateral top displacement relation is insensitive to the number of material fibres and number of elements used, i.e. mesh and element refinements do not markedly improve the response prediction (Orakcal *et al.*, 2004). This result is encouraging in that a coarse mesh can be used to assess drift responses for tall buildings, leading to reduced computer run times. However, results presented in Figure 6 present an important corollary, that use of a coarse mesh is likely to underestimate the peak strains for the material fibres (Orakcal *et al.*, 2004). The peak model compressive strains shown in Figure 6 using 8 elements and 8 fibres are approximately 30% less than the strains obtained using 17 elements and 22 fibres. Therefore, use of a fibre model with a relatively coarse mesh, although able to accurately represent the overall wall lateral load versus top displacement, may substantially under predict the maximum compressive strain at the wall critical section. For the results presented for the coarse mesh, measured peak compressive strains exceed model results by a factor of more than 2·5 (30% due to the mesh, and a factor of two from Figure 3); therefore, an acceptance criterion with a limiting peak compressive strain of 1% implies actual peak compressive strains might be closer to 2·5%. Given the information presented, acceptance criteria for wall strains should carefully consider the model attributes to establish an appropriate limit for peak concrete compression strain at critical wall locations.

Depending on the selection of the material relations and model attributes, model estimates of local deformations may be impacted by localization of inelastic deformations. For example, consider a model with a relatively large number of elements at the wall critical section and a bilinear material model with no post-yield stiffness are used to model the test wall RW2 discussed earlier (Figures 1 and 3). The yield displacement is approximately 0·5 inches; therefore, to achieve a peak top lateral displacement of 3·0 inches as observed in the test, the plastic rotation over a plastic hinge length of one-half the wall length ($l_w/2 = 24$ inches) is $\theta_p = (3{\cdot}0 - 0{\cdot}5)/(150 - 24/2) = 0{\cdot}018$. However, if an element height of 4 inches along with no material (reinforcement) strain hardening, the associated plastic curvature is $\phi_p = 0{\cdot}0018/4$ inches = 0·0045/inch and the peak wall compressive strain is estimated as $\varepsilon_{c,\max} = (\phi_y + \phi_p)(c \approx 0{\cdot}15l_w)$ or $\varepsilon_{c,\max} = (0{\cdot}003/l_w + 0{\cdot}0045)(0{\cdot}15)(48'') = 0{\cdot}033$, whereas the peak measured concrete strain in the test reached only 0·006. The strains predicted with the model are unrealistically large due to the short element height combined with the lack of post-yield stiffness, which limits yielding to only one element. Inclusion of some post-yield stiffness would allow the base moment to increase and eventually spread yielding to adjacent elements above the element at the base, and the results presented in Figures 1 and 3 indicate that this approach can produce very

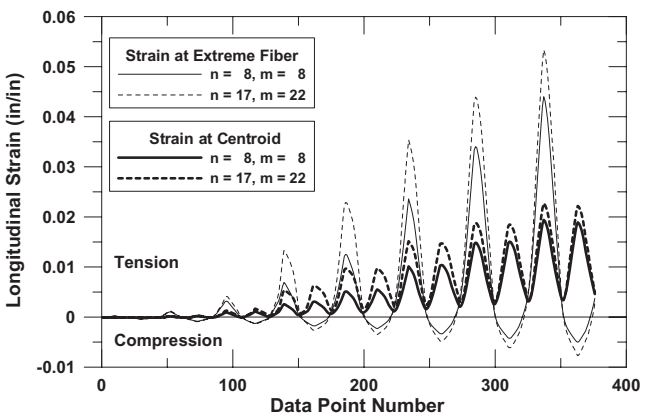

Figure 6. Wall critical strain sensitivity to model parameters

DOI: 10.1002/tal

good agreement between test and model results. However, these results are for a relatively refined mesh and fairly sophisticated material models (Orakcal and Wallace, 2006). For design, a simple approach is typically required, i.e. the element at the wall base should be selected to be approximately equal to the expected plastic hinge length, or approximately ($l_w/2$ = 24 inches). The estimated peak compressive strain for this case is $\varepsilon_{c,\max} = (\phi_y + 0{\cdot}00075/in.)(0{\cdot}15)(l_w = 48'') = 0{\cdot}006$, which is consistent with the test results. In general, the element height at the wall critical section should be approximately equal to the expected plastic hinge length and modest post yield stiffness should be used to help avoid problems associated with localization of inelastic deformations. Use of a modest reinforcement strain hardening slope of 3 to 5% is a good means to accomplish this goal. Preliminary modelling studies also indicate that use of modest strain hardening better predicts the cyclic load versus displacement response of test results (Figure 7).

Massone *et al.* (2006a, 2006b) present a modelling approach that incorporates flexure–shear interaction for monotonic loading. Details of the modelling approach are beyond the scope of this paper; however, results for the slender walls discussed earlier and shown in Figure 4 indicate that the model captures the observed interaction between flexure and shear (shear yielding not observed in uncoupled models). For the coupled analysis, larger concrete compressive strains results relative to an uncoupled analysis. A rigourous study is needed to assess the magnitude of the impact of the coupled analysis on peak compressive strains; however, the preliminary results suggest that the coupled analysis is responsible for some of the discrepancy between the wall strains predicted with an uncoupled model and the test results.

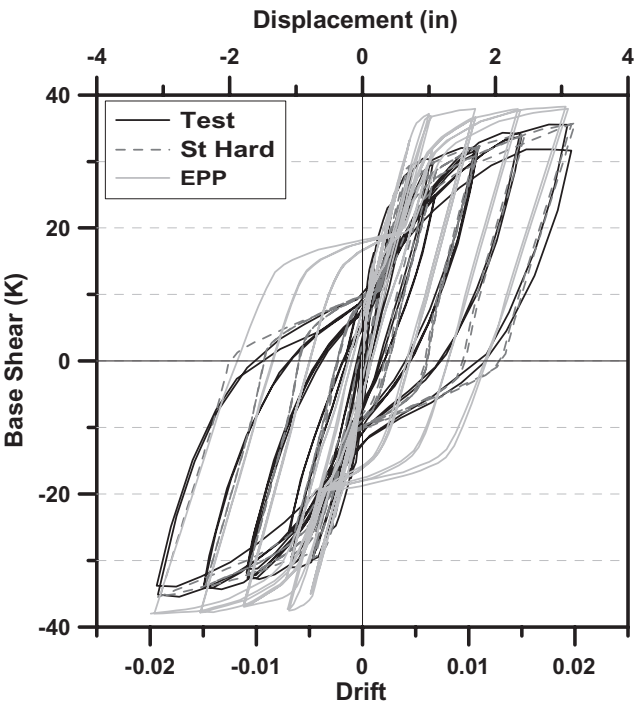

Figure 7. Model sensitivity to reinforcement properties

DOI: 10.1002/tal

3. COUPLING BEAMS

Current code provisions (ACI 318-05, 2005) for diagonally reinforced coupling or link beams produce designs with substantial congestion of reinforcement (Figure 8(a)), making them difficult and expensive to construct. New detailing provisions will be introduced in ACI 318-08 (2008) Chapter 21 to address this issue. The new provisions allow two options, one similar to prior ACI codes where transverse reinforcement is placed around the diagonal bars (Figure 8(a, b)) with modest transverse reinforcement around the entire beam section, and an alternative where a larger quantity of transverse reinforcement is provided around the entire cross-section is confined (Figure 8(c)).

A test programme is underway at University of California, Los Angeles (UCLA) to assess the response of link beams using the two options identified in ACI 318-08 (2008). The test specimens are one-half scale and the test geometries and reinforcement were selected to be representative of common conditions for residential (l_n/h = 36″/15″ = 2·4) and office (l_n/h = 60″/18″ = 3·33) construction. Diagonal reinforcement consists of a six-bar arrangement of #7 US Grade 60 reinforcing bars with expected maximum shear stresses of approximately $v_{u,max} = 6\sqrt{f'_c}$ psi and $v_{u,max} = 10\sqrt{f'_c}$ psi for the link beams with span to total depth ratios of 3·33 and 2·4, respectively. Reinforcing details for the two specimen are shown in Figure 9. To date, test results are available for four beams, two tests for span-to-depth ratios of 2·4 and 3·33 for the alternative detailing options (Figure 8). Important preliminary findings are summarized in the following paragraphs.

The shear force versus link beam rotation relations for tests with aspect ratio of 3·33 are presented in Figure 10 and reveal that very similar force deformation responses were obtained using the different detailing schemes for both aspect ratios. Rotation levels exceeding roughly 8% were achieved for all four tests with virtually no strength degradation. The peak link beam shear stress reached approximately $v_{u,max} = 6\sqrt{f'_c}$ psi (Figure 11(a)) and the force deformation loops for each beam were nearly identical, indicating that the detailing arrangement given in Figure 8(c) was as effective as that for

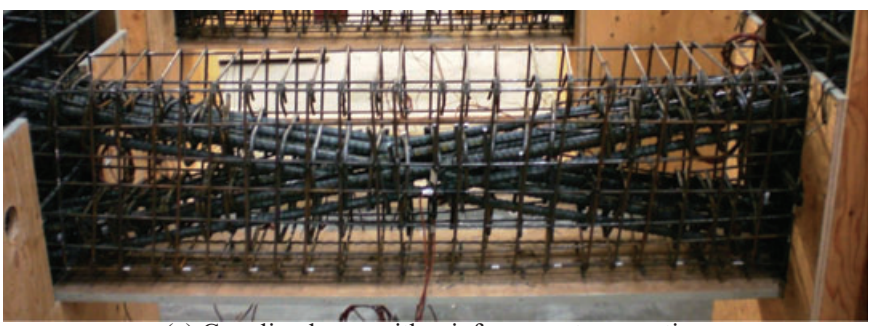

(a) Coupling beam with reinforcement congestion

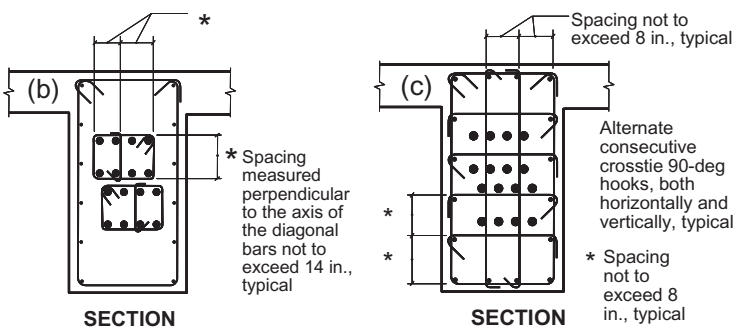

Figure 8. Link beam detailing (a) test, (b) ACI 318-05, (c) ACI 318-08 proposed

DOI: 10.1002/tal

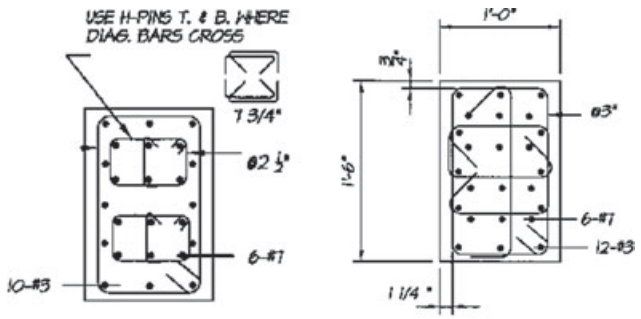

(a) ACI 318-08 Option (1) Diagonal (b) ACI 318-08 Option (2) Full

Figure 9. Link beam tests: l/h = 3·33, one-half scale

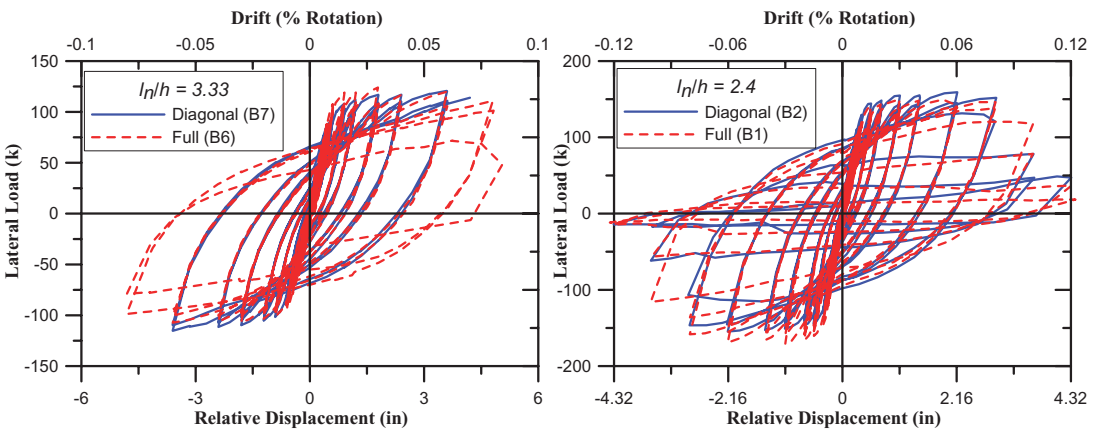

Figure 10. Load deformation relations

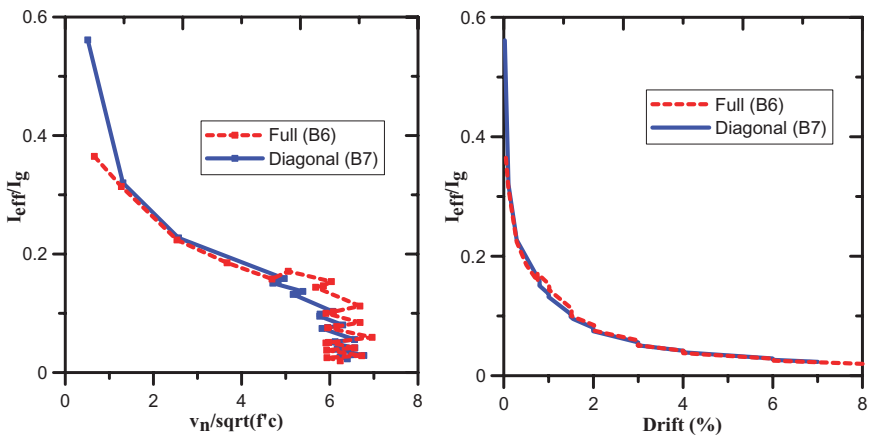

Figure 11. Effective stiffness versus (a) shear stress and (b) drift

DOI: 10.1002/tal

Figure 8(b) for this beam configuration. Figure 11(b) plots the effective secant stiffness as a fraction of concrete gross section stiffness for each test specimen and reveals an effective stiffness of approximately 0·25 to 0·40I_g for initial loading, 0·1I_g when the peak shear stress was reached at 1% rotation, 0·05I_g and 0·03I_g for 2 and 4% rotations, respectively. The relatively low initial stiffness may have been influenced by minor initial cracking that existed in the test specimens. A more thorough assessment of appropriate values for the effective moment of inertia will be conducted at the completion of the test programme.

Link beam stiffness is often reduced during the design phase to reduce link beam shear stresses to code-acceptable levels (i.e.,$v_{u,max} = 10\sqrt{f'_c}$ psi) giving rise to concerns that excessive crack widths and concrete spalling may be required to achieve the assumed stiffness values. However, the preliminary test results indicate only hairline to 1/64″ diagonal crack widths and 1/8″ to 3/16″ flexural crack widths for lateral drift levels of 3 to 4% (at the peak displacement). Residual (at zero displacement) crack widths at 4% drift were approximately 1/32″ for flexural cracks and up to 1/64″ for diagonal cracks. Photos of the 3·33 aspect ratio test specimens at several drift ratios are provided in Figure 12. Similar crack widths were observed for the shorter span to total depth ratio of 2·4, despite the higher shear stress level attained ($\approx 10\sqrt{f'_c}$ psi); however, it is noted that substantial pullout of the diagonal bars was observed. For actual buildings, the existence of a reinforced concrete slab (potentially with post-tensioning reinforcement) might restrain pullout and lead to more extensive cracking. However, preliminary results indicate that use of a reduced stiffness for link beams is unlikely to produce excessive cracking or concrete spalling, either at the service load levels or for rotation limits used for the Design Basis or Maximum Considered Earthquake levels.

As noted earlier, the use of post-tensioned slab-column frames with reinforced concrete core walls has become relatively common for tall buildings. The existence of the slab post-tensioning reinforcement will restrain the axial growth of the beam (which was unrestrained in the tests described above) and impact the test results. Therefore, link beam tests are planned in Phase II of the UCLA link beam tests to study the impact of the reinforced concrete slab, with and without post-tensioning reinforce-

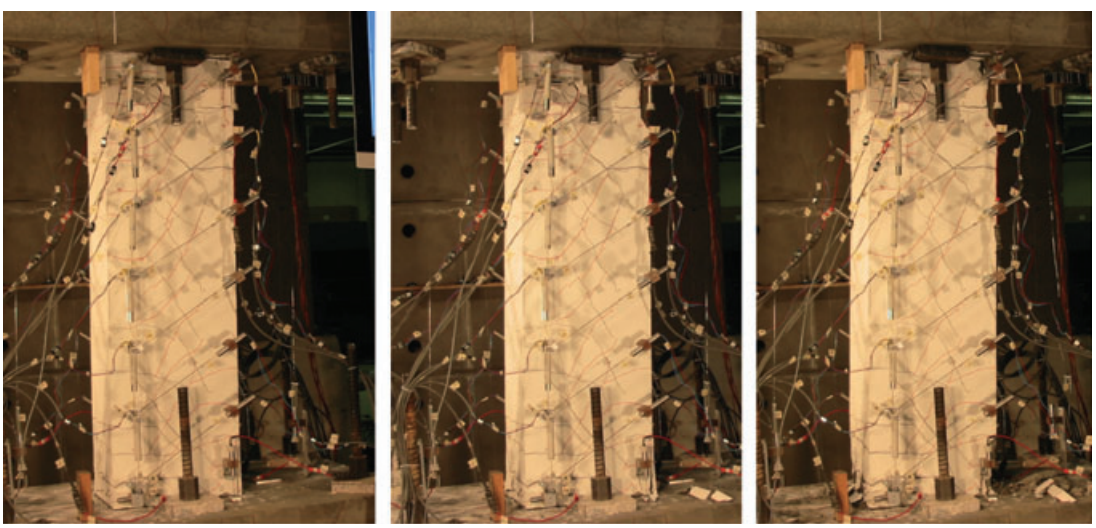

(a) 3% (b) 4% (c) 6%

Figure 12. Damage photos of Beam #7: *l*/*h* = 3·33 specimens

DOI: 10.1002/tal

ment, on link beam performance. The axial compression imposed by the post-tensioning would be expected to increase link beam strength and stiffness, and potentially reduce deformation capacity. The upcoming tests will shed important light on these issues.

4. MODELLING OF SHEAR-DOMINATED WALL SEGMENTS

Relatively limited information exists on appropriate modelling approaches for reinforced concrete wall segments with shear-dominant behaviour. A review tests results by Sozen and Moehle (1993) indicated that use of a bilinear force versus deformation relation defined by a cracking stress and a post-yield slope reasonably represented the limited test results available. Recent tests and modelling studies, although primarily conducted on lightly reinforced wall piers, provide significant data to make new recommendations as summarized in the following paragraphs.

Based on a review of test results for lightly reinforced wall piers, a force versus deformation relation based on the following points was proposed by Wallace *et al.* (2006):

$$V_{cr} = 4\sqrt{f'_c}\left[1+\frac{P_u/A_g f'_c}{4\sqrt{f'_c}}\right]^{1/2} < 0{\cdot}6V_n \quad \gamma_{cr} = \frac{V_{cr}}{0{\cdot}4E_c}$$
$$V_y = V_n = A_{cv}\left(\alpha_c\sqrt{f'_c}+\rho_n f_y\right) \quad \gamma_y = 0{\cdot}004 \tag{1}$$

As well, for lightly reinforced wall piers, shear strength degradation occurred at a deformation of approximately 0·0075 times the specimen height ($0{\cdot}0075h_w$), as described in FEMA 356 (2000). Residual strength for the piers tested by Massone (2006) was low given that the piers were lightly reinforced and generally contained poor details. Comparisons of the proposed backbone curve with experimental results for several tests are given in Figure 13.

The results presented in Figure 13(a, b) indicate that the relation defined by Equation (1) provides a reasonable fit to precracked behaviour, the nominal capacity, and the yield deformation for lightly reinforced tests with zero axial load. For the wall pier with modest axial load ($P = 0{\cdot}05A_g f'_c$) shown in Figure 13(c), the ratio of the peak load in the test to the nominal capacity using Equation (1) is roughly 1·5 and deformation associated with the yield point is less than 0·004, indicating that the axial load produces a noticeably stronger and stiffer response. However, test data for wall piers with axial load are very limited; therefore, a more detailed assessment of the influence of axial load on shear strength and yield deformation for wall piers is not possible. Until more data are available, the relation described by Equation (1) is recommended.

The modelling approach for coupled flexure–shear responses was used to compare model results with test results for several walls. Results are presented in Figure 14 and described in more detail by Massone *et al.* (2006a, 2006b) and Massone (2006). As observed in Figure 14(a), a very good correlation is obtained between test results and results of the proposed coupled shear–flexure model for Specimen 74 ($M/(Vl) = 1{\cdot}0$). Since the design flexural and shear capacities of the specimen are close, to consider the possibility that the response of the specimen is governed by nonlinear flexural deformations (i.e., the specimen does not experience significant nonlinear shear deformations), Figure 14(a) also includes an analytical flexural response prediction (with shear deformations not considered) obtained using a fibre model. The same geometric discretization and material constitutive models used in the coupled model were adopted for the fibre model, with the distinction that the panel elements (strips) of the coupled model were replaced with uniaxial (fibre) elements. Figure 14(a) illustrates that although the flexural (fibre) model provides a ballpark estimation of the wall lateral load capacity,

DOI: 10.1002/tal

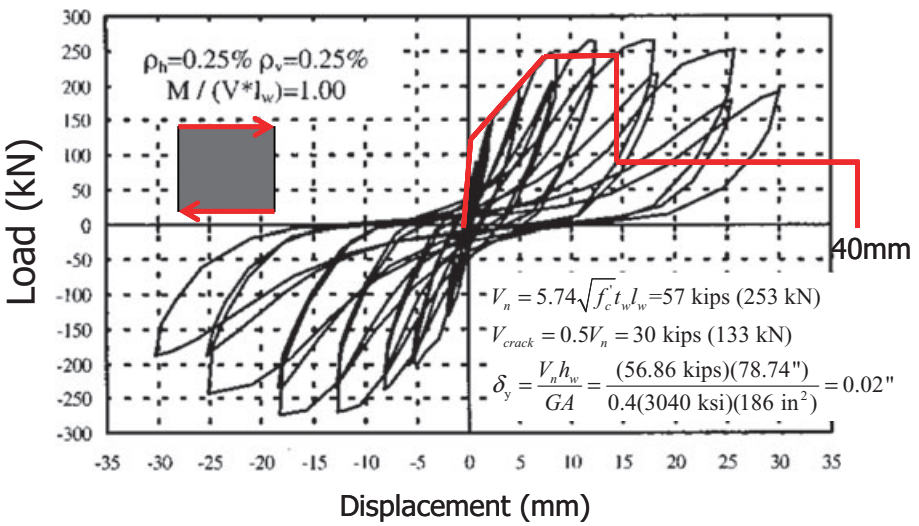

(a) Proposed shear backbone relation with test by Hidalgo et al. (2002)
(strength degradation and residual strength defined by FEMA 356 (2000))

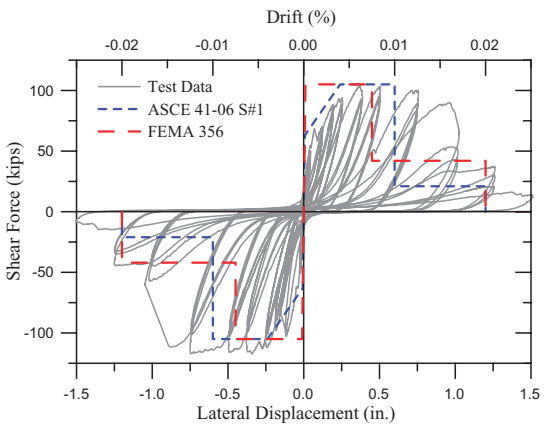

(b) Spandrel (Massone, 2006)

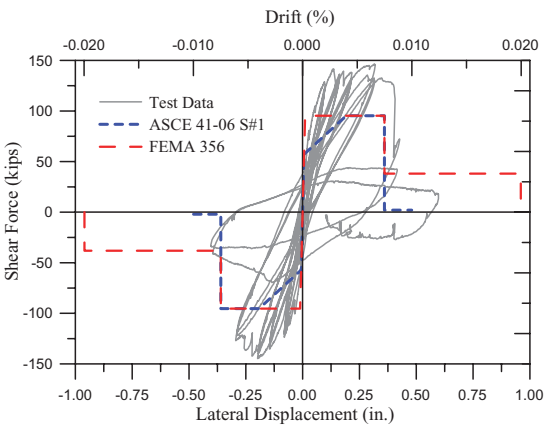

(c) Pier (Massone, 2006)

Figure 13. Wall segment force versus deformation relations

(predicted lateral load capacities approximately 750 and 980 kN, respectively, for the coupled and flexural models), the load displacement response obtained by the flexural model is significantly different from the measured response and the coupled model response. After a lateral load of 450 kN, significant lateral stiffness degradation is observed in both the test results and results of the coupled model, but not in with the flexural model.

This result demonstrates how the coupled shear–flexure model is able to simulate observed responses with substantially greater accuracy than a uncouple model, particularly for wall specimens where the nominal shear and flexural capacities are nearly equal. The correlation between results of the coupled model and test results for Specimen 10 ($M/(Vl) = 0{\cdot}69$) is similar to that of Specimen 74 (Figure 14(b)). The model provides a good prediction of the lateral load capacity and lateral stiffness of the wall

DOI: 10.1002/tal

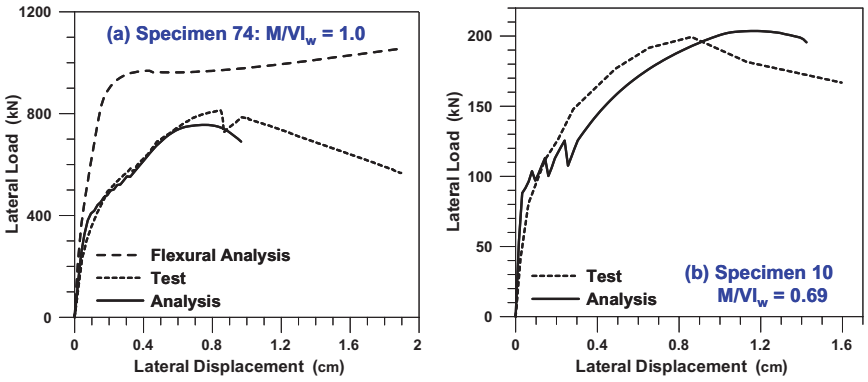

(a) $M/Vl_w = 1.0$ (b) $M/Vl_w = 0.69$ Hiwosawa (1975)

Figure 14. Coupled analysis: (a) M/Vl_w = 1·0, (b) M/Vl_w = 0·69

specimen for most of the top displacement history, although the wall specimen reaches its peak lateral load capacity at a smaller top displacement than that predicted by the model. The sudden lateral load reductions observed in the model response are due to sequential cracking of concrete, whereas such behaviour is not observed in the test results. Refining the model mesh (increasing the number of strips used along the length of the wall) would invoke a more gradual and continuous shape for the analytical load displacement response. Model predictions are not as good for walls with ($M/(Vl) > 0{\cdot}5$) because model assumptions are not appropriate for such low aspect ratio walls where the end restraint significantly impacts the wall strain distribution. Massone (2006) indicate that use of a nonlinear horizontal strain profile can be used to improve response predictions for such walls.

5. SLAB-COLUMN FRAMES

Detailed modelling information is presented in ASCE 41 Supplement #1 (Elwood *et al.*, 2007) as well as recent papers (Kang and Wallace, 2005, 2006; Kang *et al.*, 2006); therefore, only a brief overview summary of critical issues is included here.

In recent research (Kang and Wallace, 2005, 2006), use of an effective slab width model with coefficients for the elastic, uncracked effective width (α) and for cracking (β) are recommended for both reinforced concrete and post-tensioned concrete construction. The potential for punching shear failure at the slab-column connection is modelled using a rigid connection element (Kang *et al.*, 2006; Elwood *et al.*, 2007) with the connection stress limit defined using the eccentric shear stress model of ACI 318. However, given the detailed calculations required to check slab-column punching requirements, the relatively low cost of providing slab shear reinforcement (according to some engineers), as well as the improved performance that use of shear reinforcement provides (Kang and Wallace, 2005), it is fairly common to provide slab shear reinforcement at all slab-column connections without calculation (to satisfy the requirements of ACI 318-05 (2005) §21.11.5 where shear reinforcement is required).

Although it is a relatively easy process to determine slab effective widths using the approach described in the preceding paragraph for slab-column frames, and additional work has been conducted for slab-wall coupling (Qadeer and Smith, 1969; Paulay and Taylor, 1981; Wallace *et al.*, 1990), current

DOI: 10.1002/tal

practice does not consider the impact of the coupling between the slab-column frame used as the primary gravity force system and the lateral system (e.g., reinforced concrete walls). This approach is based on common practice for seismic design, where the strength and stiffness contribution of the gravity system are neglected. However, as adjustments are made to refine the effective stiffness used for walls and columns (Elwood *et al.*, 2007), as well as the impact of soil-foundation flexibility, this approach may need to be revisited for tall buildings. Parametric studies of several typical core wall configurations for various building heights would be helpful in assessing the influence of slab coupling on overall system behaviour (e.g., lateral drift, inelastic element demands and gravity system column axial loads).

6. INSTRUMENTATION FOR SEISMIC MONITORING

The boom in tall building construction also provides a unique opportunity to employ monitoring equipment to measure structural responses for a variety of conditions (ambient, high-level wind and earthquake). Ideally, a broad spectrum of sensor types capable of measuring floor accelerations, wind pressures, average concrete strains, rebar strains and rotations should be employed. In addition to a broad spectrum of sensors, key attributes of a robust monitoring system include rapid deployment, energy efficiency, event detection, robust analogue-to-digital conversion, local storage, redundant time synchronization, mulit-hop wireless data transport and remote sensor and network health monitoring. Recent developments in all of these areas reveal that robust structural health monitoring is likely to emerge over the next decade. Therefore, careful consideration should be given to increased use of sensors in existing and planned buildings. In general, more sensors are needed than are often employed in buildings, i.e. where only one triaxial accelerometer at the base, a mid-level and the roof.

Given the complexity and geometry of tall buildings, laboratory studies, which are hindered by scale, materials and appropriate boundary conditions, are unlikely to provide definitive results for a variety of important issues. For a given instrumented building, the details of the embedded sensor network design should be model-driven, i.e. sensor types and locations determined based on response quantities obtained from 3D dynamic finite element models subjected to a suite of site-specific ground motions. For example, in moment frames, response quantities of interest might be interstory displacements at several floors (where maximum values are expected) along with base and roof accelerations. In cases where novel systems or materials are employed (e.g., high-performance concrete, headed reinforcement, unbonded braces), additional instrumentation could be used to measure very specific response quantities (e.g., headed bar strain, axial deformations, etc.). In a concrete core wall system, response quantities of interest might be average core wall concrete strains within the plastic hinge (yielding) region and rotations imposed on coupling beams (or slab-wall connections). Other modelling and design issues could also be targeted, such as so-called podium effects and appropriate ground motion building inputs at subterranean levels (Stewart, 2007). Given the uncertainty associated with the response of structural systems to earthquake ground motions, a probabilistic distribution of response quantities of interest (e.g., interstory displacements, coupling beam deformations) should be determined for the structural model subjected to the suite of ground motions and the sensor layout should target specific regions versus a single response quantity.

The City of Los Angeles requires building instrumentation (accelerometers) be installed at the base, mid-level and roof to obtain a building permit for all buildings over 10 stories as well as for buildings over 6 stories with an aggregate floor area exceeding 60,000 square feet (Los Angeles Building Code §1635, 2002). The owner is required to maintain the instrumentation in working order; the City of Los Angeles has an extensive programme for monitoring the equipment currently installed in approx-

DOI: 10.1002/tal

imately 400 buildings. Currently, data collected by the required accelerometers are not typically archived and are not readily available for use either for rapid post-event assessment or by researchers to improve our ability to model buildings. Clearly, there are buildings where the measurement of interstory drift (moment frame) or average concrete strain (base of a shear wall system) might produce more useful and meaningful data than acceleration data alone. The instrumentation requirements for the City of Los Angeles are currently being updated to allow a more diverse array of sensors to provide more meaningful response quantities for very tall buildings.

7. CONCLUSIONS

An overview of some important issues associated with analysis and design of tall reinforced concrete wall buildings was presented. Based on this review, the following observations and conclusions are noted.

Existing commercially available computer programs that incorporate fibre models (or similar models) are capable of reproducing lateral load versus top displacement relations measured from moderate scale, relatively slender walls subjected to constant axial load and cyclic lateral displacements. Based on a review of test data, an effective stiffness of $0{\cdot}5I_g$ is appropriate for rectangular walls with modest axial load unless very light boundary reinforcement is used. Model element heights used within the potential plastic hinge region should be selected to be approximately equal to the anticipated plastic hinge length and a modest reinforcement strain hardening ratio of 3 to 5% should be used to avoid potential problems associated with concentration of inelastic deformations within a single element of short height. Sufficient elements and fibres should be used to ensure the strain distribution along the cross-section is adequately represented; however, even with these steps, current models underestimate the peak compressive strains measured in a limited number of tests by a factor of about two. Coupling between nonlinear flexural and shear deformations appears to be one factor that could explain this observed discrepancy.

Interaction between flexure and shear can substantially impact the load deformation response of stout walls which are common at the lower levels of tall buildings due to podium/parking levels and foundation walls. For stout walls, it is important to consider the impact of concrete cracking on the lateral stiffness. In most existing commercially available computer programs, nonlinear shear behaviour is modelled independently from axial–flexural behaviour. A modified backbone relation which defines cracking and yielding points is recommended for stout walls with low axial load. The proposed relation captures the load deformation response of lightly reinforced wall segments with very low axial load reasonably well; however, for even modest axial load levels ($P = 0{\cdot}05A_g f'_c$), the proposed model underestimates the peak strength and overestimates the yield displacement based on very limited test data.

New recommendations for modelling slab-column frame stiffness and punching failures has been incorporated into ASCE 41 Supplement #1 to assess lateral load response. As design documents incorporate more realistic estimates of component stiffness, modelling of the complete lateral and gravity systems for nonlinear response history analysis may be appropriate provided computer run times are not excessive (and continue to improve dramatically).

Given the complex issues that arise for tall buildings and the limited benefit of laboratory testing for such large structures, an aggressive programme to incorporate building instrumentation is needed. A program is underway in Los Angeles to address this need.

ACKNOWLEDGEMENTS

The work presented in this paper was supported by funds from KPFF Los Angeles Consulting Engineers, the National Science Foundation under Grant CMS-9810012, as well as in part by the

DOI: 10.1002/tal

Earthquake Engineering Research Centers Program of the National Science Foundation under NSF Award Number EEC-9701568 through the Pacific Earthquake Engineering Research (PEER) Center and The Center for Embedded Networked Sensing under the NSF Cooperative Agreement CCR-0120778. Much of the analysis and test results presented were taken from the Ph.D. dissertations of former UCLA Ph.D. students Dr Leonardo Massone, now at the University of Chile, and Dr Kutay Orakcal, now at Bogazici University, Turkey, and their collaboration and cooperation is gratefully appreciated. The participation and assistance of KPFF engineers Mr John Gavan, Mr Aaron Reynolds, Ms Ayse Kulahci and Dr Luis Toranzo on the wall segment test programme is acknowledged. The preliminary materials on the coupling beam tests will form the basis of Mr David Naish's Master's Thesis Study currently underway at UCLA. The assistance of UCLA researchers Dr Alberto Salamanca and Dr Thomas Kang are greatly appreciated. Undergraduate laboratory assistants Y. Majidi, B. Bozorgnia, J. Park, N. Lenahan, P. Navidpoor, N. Taheri and PEER summer intern Ms N. N. Lam, and Senior Development Engineer Mr Steve Keowen, also helped with the conduct of the experimental programmes. Any opinions, findings and conclusions or recommendations expressed in this paper are those of the author and do not necessarily reflect those of the supporting organization or other people acknowledged herein.

REFERENCES

ACI 318-05. 2005. *Building Code Requirements for Structural Concrete (ACI 318-05) and Commentary (ACI 318R-05)*. American Concrete Institute: Farmington Hills, MI.

ACI 318-08. 2008. *Building Code Requirements for Structural Concrete (ACI 318-08) and Commentary (ACI 318R-08)*. American Concrete Institute: Farmington Hills, MI.

Elwood K, Matamoros A, Wallace J, Lehman D, Heintz J, Mitchell A, Moore M, Valley M, Lowes LN, Comartin C, Moehle JP. 2007. Update to ASCE/SEI 41 concrete provisions. In *Proceedings*, *Los Angeles Tall Buildings Structural Design Council*, 2007 Annual Meeting, May 2007.

FEMA 356. 2000. *Prestandard and Commentary for the Seismic Rehabilitation of Buildings*, prepared by the American Society of Civil Engineers for the Federal Emergency Management Agency, Washington, DC. (FEMA Publication No. 356).

Hidalgo PA, Ledezma CA, Jordan RM. 2002. Seismic behavior of squat reinforced concrete shear walls. *Earthquake Spectra* **18**(2): 287–308.

International Building Code: IBC-2003. 2003. International Code Council.

Kang TH-K, Wallace JW. 2005. Responses of flat plate systems subjected to simulated earthquake loading. *ACI Structural Journal* **102**(5): 763–773.

Kang TH-K, Wallace JW. 2006. Punching of reinforced and post-tensioned concrete slab-column connections. *ACI Structural Journal* **103**(4): 531–540.

Kang TH-K, Elwood KJ, Wallace JW. 2006. Dynamic tests and modeling of RC and PT slab-column connections, *8th US National Conference on Earthquake Engineering*, San Francisco, April 2006, Paper 0362.

Klemencic R, Fry JA, Hurtado G, Moehle JP. 2006. Performance of post-tensioned slab-core walls connections. *PTI Journal* **4**(2): 7–23.

Los Angeles Building Code, §1635. 2002. International Code Council.

Maffei J. 2007. UCSD Building Slice Test. *Presentation*, *PEER Tall Buildings Workshop*, Task 7, 30 January 2007, San Francisco, CA.

Massone LM. 2006. RC wall shear – flexure interaction: analytical and experimental responses. PhD Dissertation, University of California, Department of Civil & Environmental Engineering, Los Angeles, CA, 398 pp.

Massone LM, Orakcal K, Wallace JW. 2006a. Shear – flexure interaction for structural walls, *8th US National Conference on Earthquake Engineering*, San Francisco, April 2006, Paper 1574.

Massone LM, Orakcal K, Wallace JW. 2006b. Modeling flexural/shear interaction in RC walls, *ACI-SP-236*, Deformation Capacity and Shear Strength of Reinforced Concrete Members under Cyclic Loadings. American Concrete Institute: Farmington Hills, MI, Paper 7, 127–150, May 2006.

Orakcal K, Conte JP, Wallace JW. 2004. Flexural modeling of reinforced concrete walls – model attributes. *ACI Structural Journal* **101**(5): 688–698.

Orakcal K, Wallace JW. 2006. Flexural modeling of reinforced concrete walls – model calibration. *ACI Structural Journal* **103**(2): 196–206.

DOI: 10.1002/tal

Orakcal K, Massone LM, Wallace JW. 2006. Analytical modeling of reinforced concrete walls for predicting flexural and coupled shear-flexural responses. *PEER Report 2006/07*, Pacific Earthquake Engineering Research Center, University of California, Berkeley, October 2006, 213 pp.

Panagiotou M, Restrepo JI. 2007. Lessons learnt from the UCSD full-scale shake table testing on a 7-story residential building slice. In *Proceedings, SEAOC Convention*, September 2007; 57–73.

Paulay T, Taylor RG. 1981. "Slab coupling of earthquake-resisting shear walls (Proceedings). *ACI Journal* **78**(2): 130–140.

PERFORM-3D. 2006. *Nonlinear Analysis and Performance Assessment for 3D Structures*, Version 4, Computer & Structures Inc.: Berkeley, CA.

Qadeer A, Smith BS. 1969. The bending stiffness of slabs connection shear walls (Proceedings), *ACI Journal* **66**(6): 464–473.

Sozen MA, Moehle JP. 1993. Stiffness of reinforced concrete walls resisting in-plane shear. Electric Power Research Institute, Research Project 3094-01, Final Report.

Stewart JP. 2007. Input motions for buildings with embedment. In *Proceedings*, *Los Angeles Tall Buildings Structural Design Council*, 2007 Annual Meeting, May 2007.

Thomsen IV JH, Wallace JW. 1995. Displacement-based design of RC structural walls: experimental studies of walls with rectangular and T-shaped cross sections. *Report No. CU/CEE-95/06*, Department of Civil and Environmental Engineering, Clarkson University, Potsdam, NY.

Thomsen IV JH, Wallace JW. 2004. Displacement-based design of slender RC structural walls – experimental verification, *Journal of Structural Engineerin*g, *American Society of Civil Engineers* **130**(4): 618–630.

Uniform Building Code: UBC-97. 1997. *International Conference of Building Officials*, Whittier, California, 1997.

Wallace JW, Moehle JP. 1992. Ductility and detailing requirements of bearing wall buildings. *Journal of Structural Engineering, American Society of Civil Engineers* **18**(6): 1625–1644.

Wallace JW, Moehle JP, Martinez-Cruzado J. 1990. Implications for the design of shear wall buildings using data from recent earthquakes. In *Proceedings*, *Vol. 2, Fourth U.S. National Conference on Earthquake Engineering*, Palm Springs, California, May 1990; 359–368.

Wallace JW, Massone L, Orackal K. 2006. St. Josephs Healthcare Orange, California SPC-2 upgrade: E/W wing component test program. *UCLA SEERL Report 2006/01*, Department of Civil and Environmental Engineering, University of California, Los Angeles, 66 pp.

DOI: 10.1002/tal